nature communications

Article

https://doi.org/10.1038/s41467-025-59308-x

Liver transplant-facilitated CD161^{+}Vα7.2^{+} MAIT cell recovery demonstrates clinical benefits in hepatic failure patients

Received: 18 January 2024

Accepted: 18 April 2025

Published online: 29 April 2025

Check for updates

Wei Wang[1,5], Chen Dai[2,5], Peng Zhu[3], Mi Wu[1], Haoquan Zhang[3], Qing Wei[4], Ting Zhou[1], Xiaosheng Tan[2], Ying Jiang[1], Xue Cheng[1], Zhihui Liang[1], Xiongwen Wu[1], Zhishui Chen[2] ✉ & Xiufang Weng[1,2,4] ✉

Mucosal-associated invariant T (MAIT) cells exert multifaceted effects such as anti-microbial activity, tissue repair, and pro-fibrotic effects across various disease settings. Nonetheless, their role in liver injury and hemostasis remains debated. Here, we report a significant depletion and functional dysregulation of MAIT cells, which is associated with disease severity and accumulated bile acids in HBV-infected patients with varying degree of liver injury. Liver transplantation facilitates a gradual recovery of recipient-originated MAIT cells. Transcriptome analysis reveals enhanced MAIT cell activation, while TCR mining demonstrates clonotype overlap between circulating and hepatic MAIT cells during significant liver injury. TCR-activated MAIT cells from transplant recipients display higher protective capacity but reduced pathological potential than those from liver failure patients. Compromised recovery of MAIT cells is linked to post-transplantation complications, whereas prompt recovery predicates favorable clinical outcome. These findings underscore the intricate interplay between MAIT cells and the hepatic environment, highlighting MAIT cells as potential therapeutic targets and sensitive predictors for clinical outcome in individuals experiencing liver failure and post liver transplantation.

Liver failure is a life-threatening clinical syndrome with high mortality and resource cost[1]. Because of the high prevalence of hepatitis B virus (HBV) infection, HBV-related decompensated cirrhosis and further developed acute-on-chronic liver failure are the most common types of liver failure in the Asia-Pacific and African regions[2]. Notably, HBV-related liver failure could develop at any stage from compensated to decompensated cirrhosis. Pathologic inflammation mediated by local immune cells plays a central role in the development of hepatic cirrhosis and subsequent liver failure[3]. Liver transplantation is currently the most efficient treatment for end-stage liver disease. In this context, many immune cells from the recipient enter the donor liver to reshape a new immune microenvironment together with the resident immune cells. Specifically, lymphoid subsets exhibiting a predilection for liver homing, such as NK cells

[1]Department of Immunology, School of Basic Medicine, Tongji Medical College and State Key Laboratory for Diagnosis and Treatment of Severe Zoonotic Infectious Disease, Huazhong University of Science and Technology, Wuhan, China. [2]Institute of Organ Transplantation, Tongji Hospital, Tongji Medical College, Huazhong University of Science and Technology; Key Laboratory of Organ Transplantation, Ministry of Education; NHC Key Laboratory of Organ Transplantation; Key Laboratory of Organ Transplantation, Chinese Academy of Medical Sciences; Organ Transplantation Clinical Medical Research Center of Hubei Province, Wuhan, China. [3]Department of Surgery, Tongji Hospital, Tongji Medical College, Huazhong University of Science and Technology, Wuhan, China. [4]Department of Transfusion, Tongji Hospital, Tongji Medical College, Huazhong University of Science and Technology, Wuhan, China. [5]These authors contributed equally: Wei Wang, Chen Dai. ✉e-mail: zschen@tjh.tjmu.edu.cn; wengxiufang@hust.edu.cn

and NKT cells, have been reported to be ready recruited into the liver from the circulation[4]. Different from NKT cells enriched in mouse liver, mucosal-associated invariant T (MAIT) cells are significantly abundant in human liver and account for up to 50% of hepatic T cells[5]. As a major intrahepatic innate-like T cell subset, both protective and pathogenic effects have been reported in various liver diseases, including anti-microbial function[5–11], immune regulatory effects[12], tissue repair potency[13–15] and pro-inflammatory effects[16]. However, the roles of MAIT cells in liver failure and post-liver transplantation remain elusive.

MAIT cells recognize the intermediate products of microbial biosynthesis of vitamin B and some small molecules, such as drug/drug-like molecules, which are presented by non-classical major histocompatibility complex-related molecule 1 (MR1)[7,17]. Human MAIT cells express a semi-invariant T-cell receptor (TCR) α chain with predominant TRAV1-2 usage[18]. However, their complementarity determining region (CDR)3β loop are highly diverse and determines the divergent responses of MAIT cells[19,20]. In addition, TCR-independent stimulations such as signals from cytokines (IL-12/IL-18) and ligands of Toll like receptors have also been shown to promote activation and functional differentiation of MAIT cells[10,21]. During the processes of HBV-related liver failure, a profound alteration of the hepatic microenvironment occurs[22], likely impacting the function of MAIT cells, either in a TCR-dependent or -independent manner. Our previous study supports this notion, revealing elevated conjugated bilirubin as a critical factor for dysregulating MAIT cells frequency and function[5]. Following liver transplantation, the restoration of liver homeostasis is expected to influence MAIT cells in the opposite direction. Conversely, functional changes in MAIT cells are likely to affect the disease or homeostasis status of the liver. However, major questions remain regarding how the interaction between MAIT cells and the hepatic microenvironment affects MAIT cell fate and liver health.

An irreversible decrease or loss of MAIT cells in the blood has been described in a series of studies, including infection[5,23,24], cancer[25,26], and autoimmune disorders[27,28], suggesting their relevance in a wide array of conditions. It remains unclear whether this is due to a systemic loss of MAIT cells or one-directional migration into tissues. Elegant studies using human tissue from biopsy and surgical resection have provided evidence for the existence of human memory T cells reside permanently in tissues that have been demonstrated in animal studies[29–31]. It has been postulated that MAIT cells do not leave tissue once they entered, because they express CXCR6 and CRTAM that confers retention in tissue but lack CCR7 and CD62L expression that is required for entering lymph nodes[32,33]. However, through chemokine receptor expression pattern and TCR repertoire comparison of MAIT cells from the blood and lymph, a recent study provides evidence to show that MAIT cells are able to exit tissue and recirculate via the lymphatics[34]. It has been reported that circulating MAIT cells in liver transplant recipients are dramatically depleted post liver transplantation, a phenomenon observed independent of the types and doses of immunosuppressive drugs employed[35]. Nonetheless, the similarities and differences of MAIT cells between blood and tissue compartments in disease settings remain poorly understood. Comparing profiles of MAIT cells in the context of liver failure and post-liver transplantation could offer valuable insights into their roles in modulating liver homeostasis.

In the current study, we demonstrate severe depletion and functional dysregulation of MAIT cells in HBV-related liver failure, which correlates with disease severity and is rescued following liver transplantation. The findings reveal that recipient-originated MAIT cells serve as highly sensitive sensors and a functional subset, allowing for the prediction of clinical outcomes and pointing towards potential therapeutic targets in individuals experiencing liver failure and post-liver transplantation.

Results

The progressive reduction of MAIT cells is associated with disease severity in liver failure patients

A cohort study was conducted to unveil MAIT cell profiling in chronic HBV-infected patients with liver failure (LF) undergoing artificial liver support or liver transplantation. Healthy donors (HD), HBV-negative carcinoid patients (HBVN), and HBV-positive patients with compensated liver function (Comp) served as controls (Supplementary Fig. 1A). MAIT cells were identified through 5-OP-RU/MR1 tetramer staining or co-staining with antibodies against CD161 and TCRVα7.2 (anti-CD161/Vα7.2) (Fig. 1A and Supplementary Fig. 1B–D). 5-OP-RU/MR1 tetramer-positive T cells and anti-CD161/Vα7.2 co-stained T ($CD161^+Vα7.2^+$ MAIT) cells exhibited consistent decreases in the blood and liver of LF patients compared to HD, HBVN, and Comp groups (Fig. 1B–D), showing a predominant CD8-positive population (Supplementary Fig. 1B).

Albeit the frequencies of circulating (cMAIT) and hepatic MAIT (hMAIT) cells from the Comp group already reduced as compared to those from HD or HBVN, MAIT cells further decreased and displayed a higher apoptosis rate in liver failure patients (Supplementary Fig. 2A and B). Of note, cMAIT and hMAIT frequencies reduced to a greater extent in liver failure patients presenting with larger liver necrotic areas (Fig. 1E), more frequent cholestasis (Supplementary Fig. 3A and B), higher scores of model for end-stage liver disease (MELD) prioritizing patients for liver transplant (Fig. 1F), higher value of histological activity index (HAI) reflecting tissue necroinflammation (Supplementary Fig. 3C), and/or multiple complications (Supplementary Fig. 3E). In contrast, nucleos(t)ide analogs therapy showed little effect on MAIT cell frequencies in liver failure patients (Supplementary Fig. 3D). These fundings suggest that the marked reduction of MAIT cell is associated with disease severity rather than therapeutic intervention in HBV-related liver failure patients.

MAIT cell depletion and impaired responsiveness are restored following liver transplantation

To access the dynamic changes of MAIT cells post liver transplantation, we proceeded to monitor the $CD161^+Vα7.2^+$ cMAIT frequencies from pretransplant to various time points posttransplant. Among the 46 recipients undergoing liver transplant enrolled in this study, 28 individuals followed a prospective cohort study for circulating MAIT cells (cMAIT-LT) monitoring in liver transplant recipients. We found that cMAIT-LT frequencies continued to decline within the first week posttransplant in most patients (Fig. 2A, B and Supplementary Fig. 3F), whereas their apoptosis rate did not increase (Supplementary Fig. 2C). The frequency of circulating MAIT cells gradually increased thereafter, with a significant increase at around 30 days post-transplantation (Fig. 2A, B). Long-term follow-up revealed that the frequency of MAIT cells at 1-year post-transplantation was even higher than pre-transplant levels and approached those seen in HD, as observed in 10 participants who completed a follow-up period of at least 1 year (Fig. 2C).

No significant change in the $CD161^+Vα7.2^+$ cell ratio was observed at different time points post liver transplantation (Fig. 2D), supporting the gradually recovery of $CD161^+Vα7.2^+$ MAIT cells post-transplant as a genuine phenomenon rather than an effect of CD161 downregulation. However, the dynamic changes of MAIT cells post-transplant were limited to $CD161^+Vα7.2^+$ cells, and some contamination of non-MAIT T cells cannot be excluded due to the broader anti-CD161/Vα7.2 gating than MR1-tetramer gating of MAIT cells. In line with the finding that changes in MAIT cell post liver transplantation are largely independent of the type and dosage of immunosuppression[35], we observed mild changes in groups receiving various immunosuppression regiments (Supplementary Fig. 4A). Furthermore, there was little correlation between MAIT cell numbers and the dosage of Tacrolimus administered to all patients post liver transplantation (Supplementary Fig. 4B).

https://doi.org/10.1038/s41467-025-59308-x

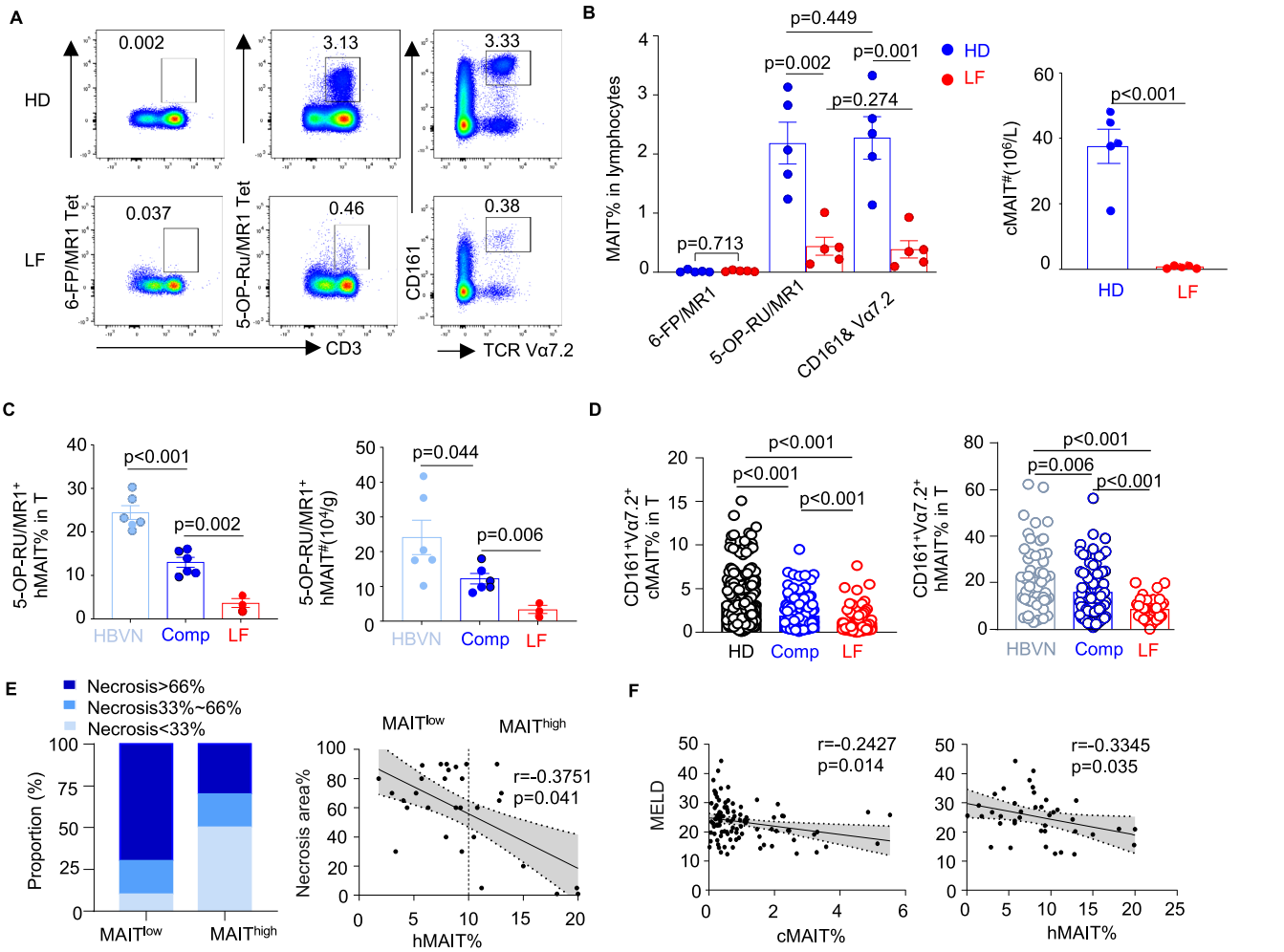

Fig. 1 | MAIT cell ratios negatively correlate with disease severity in HBV-related liver failure. A, **B** Representative plots (**A**) and summarized graph (**B**, **left panel**) for MAIT cell staining by 6-FP/MR1 tetramer, 5-OP-RU/MR1 tetramer, and/or anti-CD161/TCRVα7.2 antibodies from healthy donors (HD, $n = 5$) and liver failure patients (LF, $n = 5$). Summarized graphs (**B**, **right panel**) of the numbers of circulating MAIT cells (cMAIT) from HD ($n = 5$) and LF ($n = 5$). Statistical significance was assessed by the two-sided student's t test. **C** Summarized graphs of frequencies and numbers of hepatic MAIT cells (hMAIT) staining by 5-OP-RU/MR1 tetramer from HBV negative carcinoid patients (HBVN, $n = 6$), chronic hepatitis B patients with compensated liver function (Comp, $n = 6$), and liver failure patients (LF, $n = 3$). Statistical significance was assessed by a two-sided unpaired t test between the two groups. **D** Summarized frequencies of circulating $CD161^{+}TCRV\alpha7.2^{+}$ MAIT cells (cMAIT) in T from HD ($n = 292$), Comp ($n = 180$) and LF ($n = 107$) and frequencies of hMAIT from HBVN ($n = 50$), Comp ($n = 70$) and LF ($n = 42$). Statistical significance was assessed by the Kruskal-Wallis test followed by Dunn's test. **E** The proportion of liver failure patients with different degree of necrosis in groups with MAIT cell frequencies higher than 10% ($MAIT^{high}$, $n = 10$) and lower than 10% ($MAIT^{low}$, $n = 20$) (**left panel**); Spearman correlation between frequencies of hMAIT and necrosis areas of liver tissue from liver failure patients ($n = 30$, **right panel**). **F** Spearman correlation between the scores of the model for end-stage liver disease (MELD) and ratios of cMAIT ($n = 102$) and hMAIT ($n = 40$) from liver failure patients. Data are presented as mean ± SEM. n-values represent biological replicates. Source data are provided as a Source Data file.

To assess the TCR-dependent MAIT cell responsiveness, artificial antigen-presenting cells (aAPCs) were prepared by microbeads coating with 5-OP-RU/MR1 tetramer and anti-CD28 monoclonal antibody (mAb) to stimulate MAIT cells with supplemental IL-2 (Fig. 2E). 5-OP-RU/MR1 aAPCs specifically expanded MAIT cells but not non-MAIT T cells (Supplementary Fig. 5). Although the expansion of MAIT cells from liver failure patients was obviously dampened, MAIT cells from the liver transplant recipients proliferated and expanded sufficiently as those from healthy donors (Fig. 2F). Thus, these data reflect the reduction of MAIT cells in LF is gradually rescued post liver transplantation, accompanied by a restoration of impaired TCR-dependent proliferation.

The proinflammatory profiles and diminished anti-virus potency of MAIT cells in patients with liver failure are rectified after liver transplantation

Flow-cytometric sorted circulating MAIT cells (cMAIT-HD) and $CD8^{+}$ non-MAIT cells ($cCD8^{+}$ non-MAIT-HD) from 3 HD were subjected to bulk RNA sequencing and transcriptome analysis (Supplementary Fig. 6A). Differentially upregulated genes with log2 fold-change values greater than 1 in cMAIT-HD versus cCD8+ non-MAIT-HD were significantly enriched for pathways related to T cells activation, response to virus, and tissue repairment (Supplementary Fig. 6B and Supplementary Data 6.1). Although GESA-GO enrichment did not reveal significant results for most of these pathways, it did show reduced proinflammatory IL-6/IL-8/neutrophil-related processes (Supplementary Fig. 6C and Supplementary Data 6.2). This suggested that MAIT-cells exert overwhelming protective effects against pathogenic inflammatory responses. Nonetheless, circulating MAIT cells from LF patients (cMAIT-LF) exhibited upregulated transcript signatures linked to tissue repair and proinflammatory pathways as compared to cMAIT-HD, accompanied by a trend towards downregulation without statistical significance in processes related to virus defense. This was consistent with the findings for hepatic MAIT cells from LF patients (hMAIT-LF), which exhibited increased expression of tissue repair gens

https://doi.org/10.1038/s41467-025-59308-x

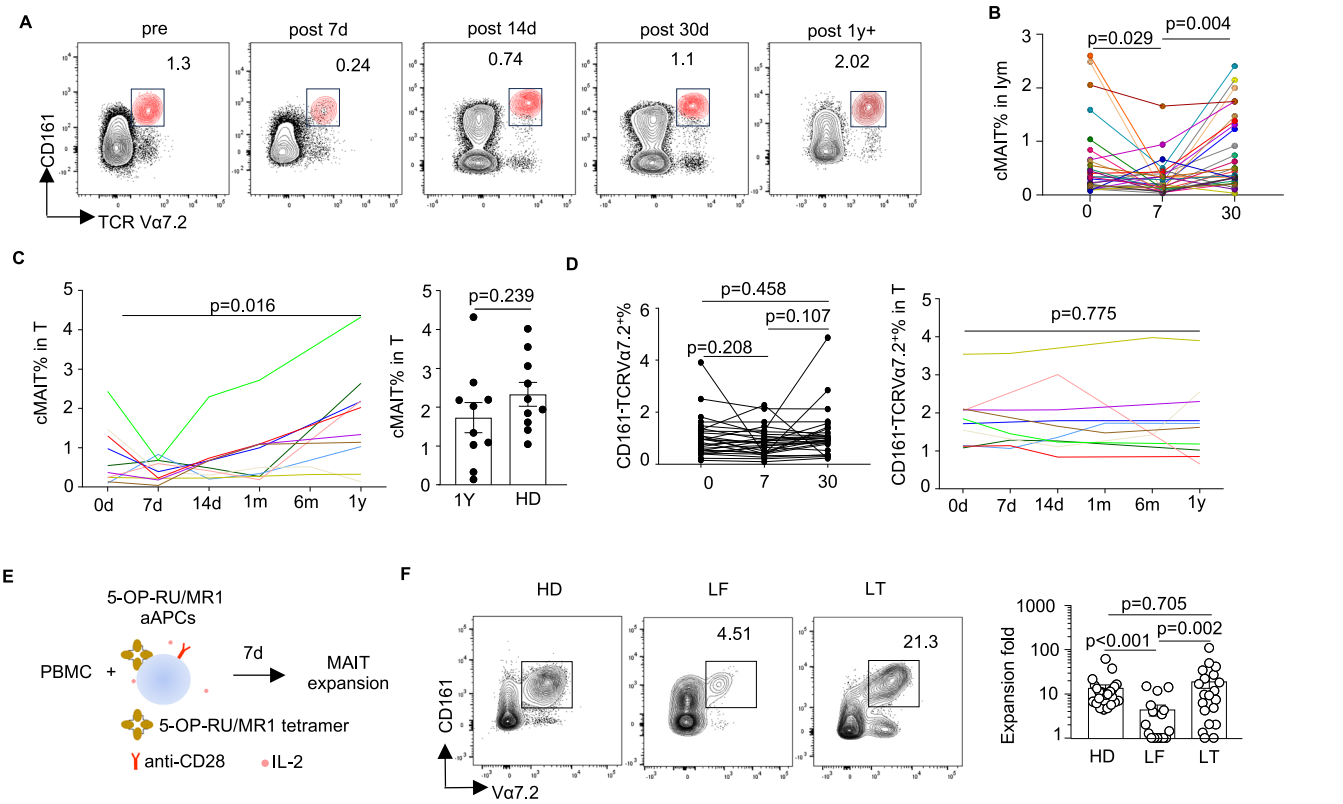

Fig. 2 | The frequencies and expansion ability of circulating MAIT cells from LF patients are gradually recovered after liver transplant. A, **B** Representative plots (**A**) and summarized frequencies (**B**) of circulating MAIT(cMAIT) from liver transplanted (LT) recipients in indicated time points ($n = 28$/group). Statistical significance was assessed by a two-sided paired Student's t test. **C** The dynamic changes of the frequencies of cMAIT cells in LT recipients of 1-year follow-up are exhibited by a line chart (**left panel**, $n = 10$). Summarized graphs (**right panel**) of the frequencies of cMAIT cells from LT 1 year post ($n = 10$) and HD ($n = 10$). Statistical significance was assessed by a two-sided paired Student's t test. **D** Summarized frequencies of circulating CD161$^-$TCRVα7.2$^+$ cells from liver transplanted recipients in indicated time points (**left panel**, $n = 28$/group) and the dynamic changes of the frequencies of CD161$^-$TCRVα7.2$^+$ cells in LT recipients of 1 year follow-up are exhibited by a line chart (**right panel**, $n = 10$). Statistical significance was assessed by a two-sided paired Student's t test. **E** Flow chart of MAIT cell expansion from PBMCs stimulated upon antigen-presenting cells (aAPCs) loaded with 5-OP-RU/MR1 in the presence of IL-2. **F** Representative frequencies (**left panel**) and expansion fold (**right panel**) of circulating MAIT cell expansion from PBMCs in HD ($n = 24$), LF ($n = 16$), and LT ($n = 20$) groups. Statistical significance was assessed by the Kruskal-Wallis test followed by Dunn's test. Data are presented as mean ± SEM. n-values represent biological replicates. Source data are provided as a Source Data file.

and a trend towards enhanced proinflammatory responses, concomitant with decreased gene expression involved in virus defense (Fig. 3A, Supplementary Fig. 6D, Supplementary Data 5.1, and Supplementary Data 6.2). In line with this, both cMAIT-LF and hMAIT-LF demonstrated reduced production of anti-viral IFN-γ (Fig. 3B and Supplementary Fig. 7). We observed increased IL-17A-producing cells in cMAIT and hMAIT of LF groups as compared to controls, albeit there appeared to be a shift in the IL-17A negative population in the liver failure patients, which would lead to an overestimation in the frequency of IL-17A$^+$cells. These findings provide evidence for the compromised antiviral function and an augmented potential for bystander pathogenic inflammation in MAIT cells from liver failure patients. Following liver transplantation over a 2-week period, there was a restoration of IFN-γ-producing capacity in MAIT cells, accompanied by a decrease in the previously aberrantly increased IL-17 production in the recipients compared to the same individuals pretransplant (Fig. 3C, D). A mild correlation between Tacrolimus dosage and IFNγ-producing capacity of MAIT cells was observed, suggesting a minimal impact of immunosuppression therapy on MAIT cells posttransplant (Supplementary Fig. 4C).

In addition to promoting their expansion, 5-OP-RU/MR1 aAPCs specifically activate MAIT cells to produce various cytokines in a TCR-dependent manner. The stimulation of MAIT cells in PBMCs from healthy donors resulted in a significant production of IFN-γ and IL-17, consistent with the predominant cytokines produced by MAIT cells. In liver failure group, there was a notable decrease in IFN-γ secretion, coupled with higher production of IL-6, MCP-1 and IL-17 in response to 5-OP-RU/MR1 aAPCs (Fig. 3E). Although bystander non-MAIT cells might contribute to the differences in cytokines in the culture, the results reflected the pro-inflammatory potential of MAIT cells, either directly through cytokine production or indirectly by influencing bystander cells. Of note, MAIT cells from liver transplantation recipients experienced a recovery in IFN-γ secretion and a reduction in proinflammatory IL-6/MCP-1/IL-17 production, bringing them to levels comparable to those of healthy controls (Fig. 3E). Collectively, these results demonstrate the rectification of MAIT cell function from liver failure-associated dysregulation after liver transplantation.

The diminished liver homing receptors CCR6/CXCR6 on MAIT cells in liver failure patients is restored following liver transplantation

In order to further analyze the characteristics of MAIT cells in the LF patients, we purified MAIT cells from different groups through flow cytometry for bulk RNA sequencing, including circulating MAIT cells from 6 HD (cMAIT-HD) and 3 LF patients (cMAIT-LF), and hepatic MAIT cells from 2 HBVN individuals (hMAIT-HBVN), 4 Comp patients (hMAIT-Comp), and 3 LF patients (hMAIT-LF). After PCA analysis of transcript signatures, we found that cMAIT-LF clustered closer to

https://doi.org/10.1038/s41467-025-59308-x

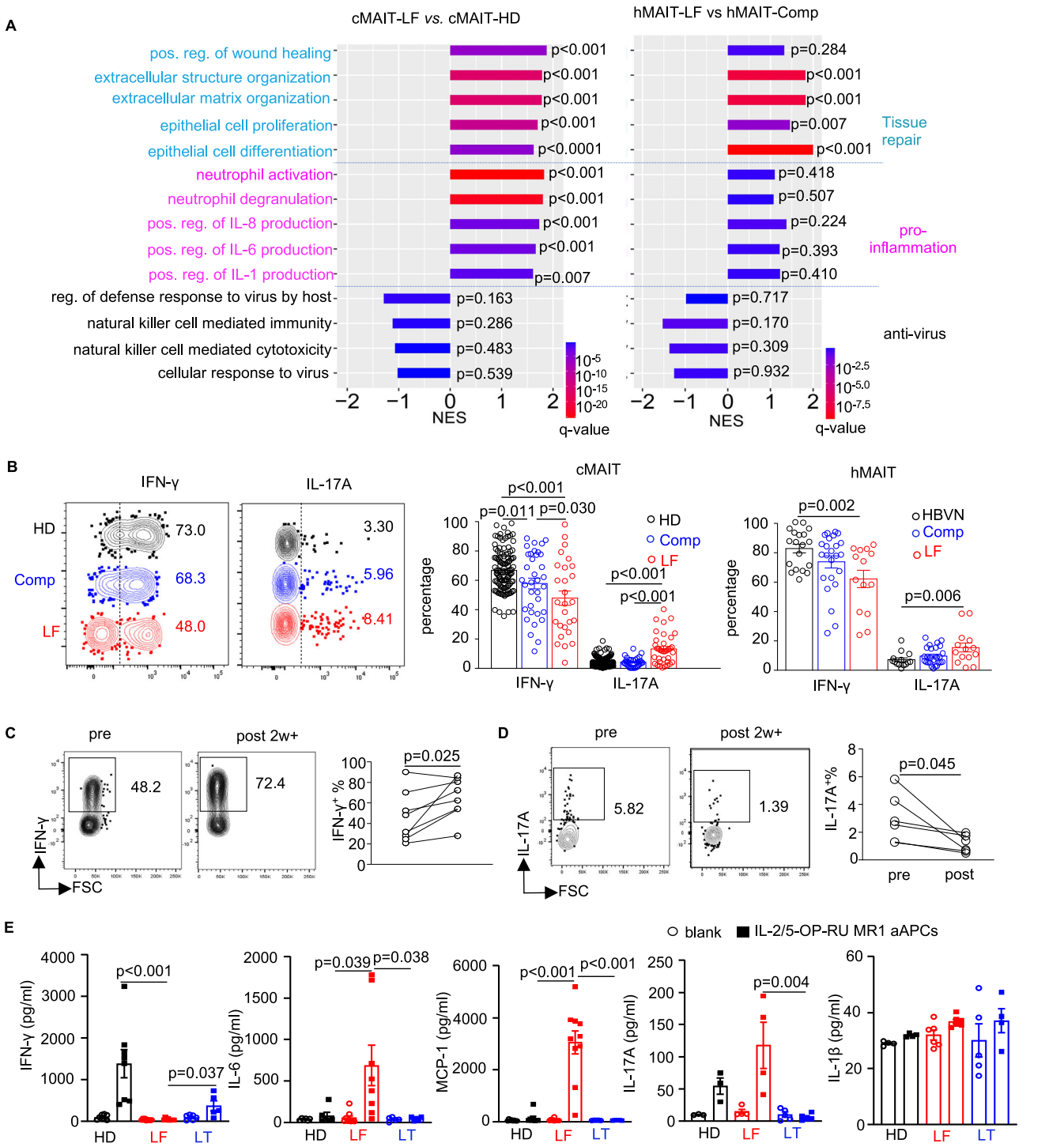

Fig. 3 | MAIT cells exhibit dysregulated functionality in liver failure patients that is rectified post liver transplantation. A Normalized enrichment scores (NES) of tissue repair-, pro-inflammation- and anti-virus-related biological processes from gene set enrichment analysis (GSEA) based on gene ontology (GO) database in cMAIT-LF ($n = 3$) versus cMAIT-HD ($n = 6$) (**left**), and hMAIT-LF ($n = 3$) versus hMAIT-Comp ($n = 4$) (**right**). **B** Frequencies of IFN-γ/IL-17A-producing cells in cMAIT-HD (IFN-γ ($n = 116$), IL-17A ($n = 193$)), cMAIT-Comp (IFN-γ ($n = 35$), IL-17A ($n = 34$)) and cMAIT-LF (IFN-γ ($n = 27$), IL-17A ($n = 36$)), and in hMAIT-HBVN (IFN-γ ($n = 19$), IL-17A ($n = 14$)), hMAIT-Comp (IFN-γ ($n = 24$), IL-17A ($n = 26$)) and hMAIT-LF (IFN-γ ($n = 14$), IL-17A ($n = 14$)) upon Phorbol 12-myristate 13-acetate(PMA)/ Ionomycin (Ion) stimulation. Statistical significance was assessed by a one-way ANOVA test followed by Fisher's LSD test. Data are presented as mean ± SEM. **C**, **D** Frequencies of IFN-γ- (**C**) and IL-17A (**D**)-producing cells of cMAIT cells from pretransplant (IFN-γ ($n = 8$), IL-17A ($n = 6$) and posttransplant (IFN-γ ($n = 7$), IL-17A ($n = 6$)) upon PMA/Ion stimulation. Data were collected from at least six independent experiments. Data are presented as mean ± SEM. Statistical significance was assessed by the two-sided paired Student's *t* test. **E** Concentration of indicated cytokines of the supernatant from unstimulated or 5-OP-RU/MR1 aAPCs-stimulated PBMCs from HD, liver failure patients, and LT recipients ($n \geq 3$/group). Data were collected from at least three independent experiments. Data are presented as mean ± SEM. *n*-values represent biological replicates. Statistical significance was assessed by a one-way ANOVA test followed by Fisher's LSD test. Source data are provided as a Source Data file.

https://doi.org/10.1038/s41467-025-59308-x

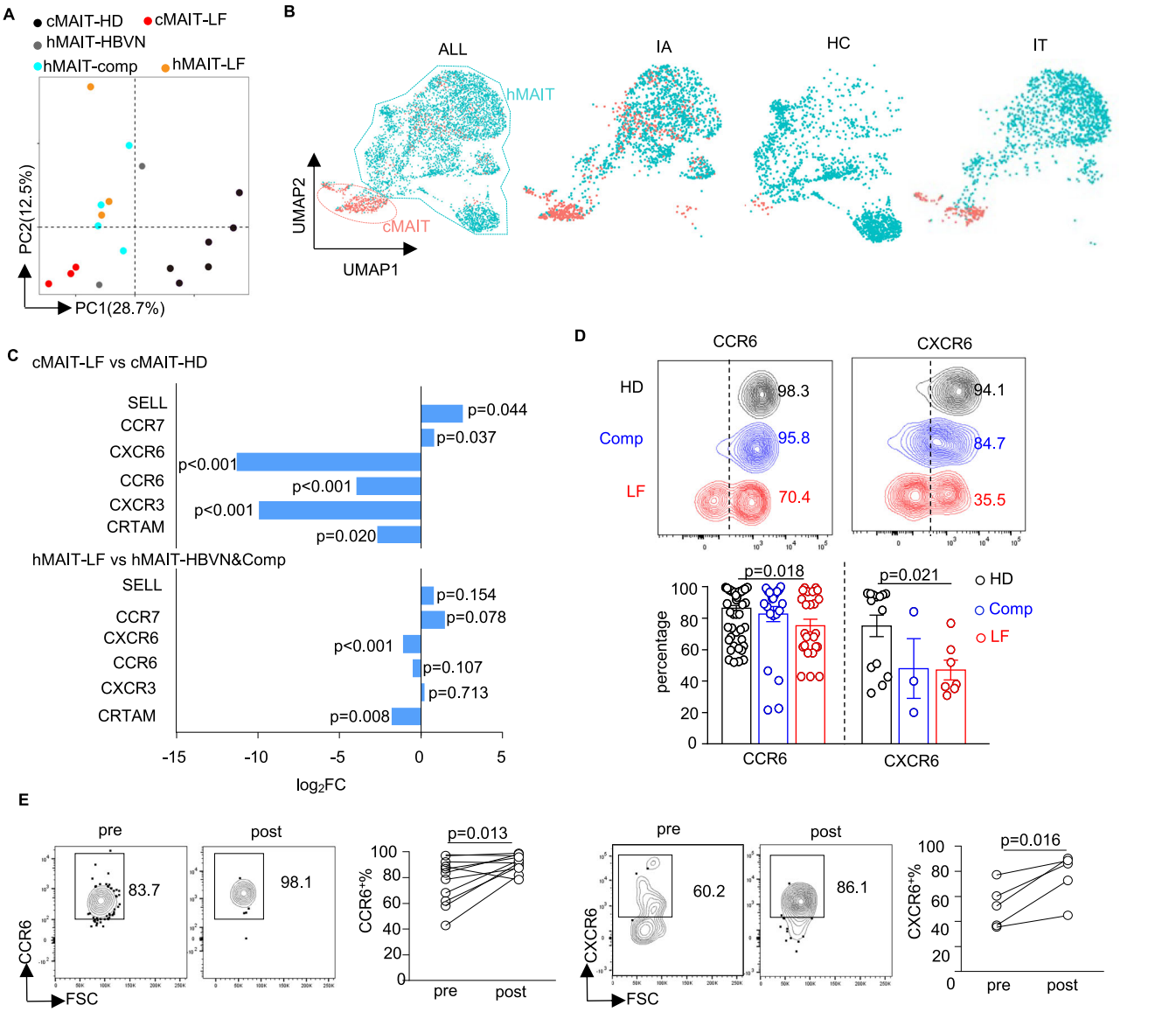

Fig. 4 | Enhanced trafficking between circulating and hepatic MAIT cells in the liver failure patients and liver transplant recipients. A Principle component analysis (PCA) clustering based on transcriptome of cMAIT-HD ($n = 6$), cMAIT-LF ($n = 3$), hMAIT-HBVN ($n = 2$), hMAIT-Comp ($n = 4$), and hMAIT-LF ($n = 3$). **B** Uniform manifold approximation and projection (UMAP) clustering plots (upper panel) for distribution of the cMAIT and hMAIT from healthy control (HC, $n = 6$), immune active (IA, $n = 5$), and immune tolerant (IT, $n = 6$) groups sourced from dataset GSE182159. **C** The relative transcription levels (log_2FC) of indicated genes in cMAIT-LF ($n = 3$) versus cMAIT-HD ($n = 6$), and hMAIT-LF ($n = 3$) versus hMAIT-HBVN($n = 2$) & Comp($n = 4$). **D** CCR6 and CXCR6 levels of cMAIT-HD (CCR6 ($n = 62$), CXCR6 ($n = 14$)), cMAIT-Comp (CCR6($n = 24$), CXCR6 ($n = 3$)), and cMAIT-LF (CCR6($n = 24$), CXCR6 ($n = 7$)). Data were collected from at least three independent experiments. Statistical significance was assessed by a one-way ANOVA test followed by Fisher's LSD test. **E** The level of CXCR6 ($n = 5$) and CCR6 ($n = 14$) of cMAIT pretransplant and around 1-week posttransplant. Data were collected from at least five independent experiments. Data are presented as mean ± SEM. *n*-values represent biological replicates. Statistical significance was assessed by the two-sided paired Student's *t* test. Source data are provided as a Source Data file.

hMAIT-LF, hMAIT-HBVN and hMAIT-Comp, but were more distant from cMAIT-HD (Fig. 4A). We next performed a secondary analysis of the published single-cell RNA sequencing dataset including paired liver and blood samples from immune active (IA) characterized by abnormal liver necroinflammation, fibrosis and serum ALT level, immune tolerance (IT) characterized by high-serum HBV DNA but normal serum ALT and mostly normal liver histology, and HBV-free healthy controls (HC) (GSE182159)[36]. Consistent with the reported transcriptomic differences between blood and liver MAIT cells[37,38], the disparate distribution of circulating and hepatic MAIT cells in uniform manifold approximation and projection (UMAP) clustering supported that distinct tissue origins play a crucial role in shaping MAIT transcript signatures (Fig. 4B). However, we observed that more cMAITs from the IA group exhibited hMAIT transcript profiling, indicating a consistent increase in transcript signatures of circulating MAIT cells similar to hepatic MAIT cells. In addition, the DEGs and the top 20 Go biological processes associated with these DEGS in circulating MAIT cells from the IA group, compared to the IT groups, were primarily related to T cell activation and cell adhesion pathways (Supplementary Fig. 8, Supplementary Data 5.2, and Supplementary Data 6.3). This indicates a heightened activation state and cellular interaction capability in MAIT cells within the IA group.

Through analysis of bulk RNA sequencing dataset from sorted MAIT cells, we observed that cMAIT-LF and hMAIT-LF from LF patients showed a trend toward upregulating *SELL* (CD62L) and *CCR7* transcripts that reflected the enhanced capacity of recirculation via

lymph, while downregulating *CXCR6*, *CCR6*, *CXCR3,* and *CRTAM* that are tissue homing receptors and retention molecules[34] (Fig. 4C, Supplementary Fig. 9A, B, and Supplementary Data 5.1). Notable, *SELL* and *CCR7* were significantly upregulated only in cMAIT-LF versus cMAIT-HD, whereas *CXCR6* and *CRTAM* were significantly downregulated in hMAIT-LF versus hMAIT-HBVN&Comp (Supplementary Fig. 9C). Flow cytometric analysis revealed the consistently reduced levels of CXCR6 and CCR6 in cMAIT-LF compared to cMAIT-HD (Fig. 4D). Of note, 5-OP-RU/MR1 tetramer$^+$ MAIT and CD161$^+$Vα7.2$^+$ MAIT cells from LF group exhibited similar decrease in CCR6 and CXCR6 levels (Supplementary Fig. 10). Following liver transplantation, recipients exhibited a restoration of CXCR6 and CCR6 expression on MAIT cells around one week, compared to pretransplant levels in the same individuals (Fig. 4E). Collectively, our results show a reduction in liver homing receptor expression on MAIT cells in liver failure patients, which was subsequently restored following liver transplantation.

Significant TCR overlapping clonotypes of circulating and hepatic MAIT cells in liver failure patients

To further access the overlapping MAIT cell clones between blood and liver tissue, we next analyzed TCR clonotypes of circulating and hepatic MAIT cells among immune active, immune tolerance, and healthy control groups sourced from dataset GSE182159. According to the expression level of canonical markers TRAV1-2 and SLC4A10, MAIT cells were identified for subsequent detailed analysis. They were consistently characterized by a semi-invariant TCRα chain with predominant TRAV1-2 and TRAJ33, paired with an array of TCRβ chain including TRBV20-1 and TRBV6 families across different disease statuses (Fig. 5A and Supplementary Fig. 11). Despite this, a notable diversity in MAIT cell TCR arises from variations in the TCRVβ chain and significant variations in the complementarity-determining regions 3 (CDR3) sequences of both TCRα and TCRβ chain (Fig. 5B). Consequently, there were prevalent MAIT cell clones exhibiting unique paired CDR3α and CDR3β sequences in both blood and liver (Fig. 5C), contributing to a high TCR diversity as assessed by the Shannon equitability index within all three groups (Fig. 5D). These results suggested that the degree of MAIT TCR diversity among the three groups differed little.

To gain a more detailed understanding of the clonal relationship between circulating and hepatic MAIT cells in different groups, we checked whether the expanded MAIT cells with clone frequencies over 5 had TCR overlapping counterparts in the liver and blood. Given the technical limitations, we observed limited numbers of expanded circulating MAIT cell clonotypes in HD and IT groups (Supplementary Fig. 12). However, notable MAIT cell clonotypes were found to be distributed bilaterally in blood and liver in IA groups with significant liver injury (Fig. 5E), demonstrating clonotype overlap between circulating and hepatic MAIT cells.

Elevated hepatic bile acid components and pro-inflammatory cytokines correlate with impaired MAIT cell expansion and/or CXCR6 expression in liver failure patients

As an innate-like T cell population, MAIT cells rapidly sense the environmental metabolites and cytokine changes. Biomarkers indicating liver injury increased significantly in liver failure patients and reduced to relatively normal level in LT recipients (Supplementary Fig. 13A). Aberrant bile acid transporting and metabolic processes accompanied with elevated pro-inflammatory processes observed in the failure liver were restored towards physical status in the transplanted liver (Supplementary Fig. 13B, Supplementary Data 5.3, and Supplementary Data 6.4). Hepatic metabolites in liver failure patients were obviously different from the control group, with predominantly upregulated metabolites in the failure liver, including taurochenodesoxycholic acid (TCDCA), glycochenodeoxycholic acid (GCDCA), and glycoursodeoxycholic acid (GUDCA) (Supplementary Fig. 13C–E and Supplementary Data 4). In line with the reversed correlations between serum bile acid levels with frequencies of cMAIT and hMAIT in liver failure patients (Fig. 6A), a trend of negative associations without statistical significance was also observed between hMAIT frequency with hepatic TCDCA, GCDCA and GUDCA levels (Fig. 6B). Moreover, transcriptional levels of *CXCL8, IL1B, IL6*, and *IL7* were upregulated (Supplementary Fig. 13F, and Supplementary Data 5.3), which were positively correlated to hepatic TCDCA, GCDCA and GUDCA levels but tended to be negatively correlated to hMAIT frequency (Fig. 6B).

Exogenous GCDCA and GUDCA rather than TCDCA inhibited MAIT cell expansion in a dose-dependent manner with a 50% inhibitory concentration (IC50) lower than 50 μM (Supplementary Fig. 14A and Fig. 6C, D). Little effect on MAIT cell apoptosis by GCDCA and GUDCA was observed, although GCDCA elevated activation marker CD38 in MAIT cells (Supplementary Fig. 14B–D). IL-1β (10 ng/mL), IL-6 (50 ng/mL), IL-7 (50 ng/mL) and IL-8 (50 ng/mL) had negligible effects on the expansion of MAIT cells upon 5-OP-RU/MR1 aAPCs stimulation (Fig. 6E). In keeping with the reported pro-inflammatory role of bile acids[39], GCDCA enhanced IL-6 production but inhibited IFN-α2 and IFN-γ releasing. All three bile acid components suppressed IFN-γ secretion, while TCDCA increased IL-33 secretion in the supernatant of 5-OP-RU/MR1-stimulated PBMCs (Supplementary Fig. 14E). Intriguingly, consistent with the overall reduction of liver homing receptors in MAIT cells from liver failure patients, the administration of TCDCA, GUDCA, IL-1β and IL-7 resulted in a decrease in CXCR6 level of MAIT cells (Fig. 6F), which was supposed to downregulate liver homing but upregulate liver exit. Taken together, our results suggest that the harsh microenvironment, such as accumulated bile acids and pro-inflammatory cytokines in liver failure patients, synergistically promotes MAIT cell dysregulation in frequency, cytokine production, and CXCR6 expression.

Recipient-originated MAIT cells are endowed with restored protective potential followed liver transplantation

To ascertain whether the recovered circulating MAIT cells originated from the donor liver or liver transplant recipients themselves, we enriched 5-OP-RU/MR1-expanded MAIT cells in PBMCs from liver transplant recipients (eMAIT-LT) around 1-month post transplantation. Subsequently, we compared their HLA alleles with those of the failure liver (FL) and transplanted liver (TL) through HLA allele genotyping using arcas-hla on bulk RNA sequencing data of liver specimens from both the donor and recipient, as well as sorted MAIT cells. The HLA alleles of eMAIT-LT cells were identical to those of failure liver (FL) from recipients but differed from the transplant liver (TL) from donors (Fig. 7A and Supplementary Fig. 15A). This reflected that the recovered circulating MAIT cells were derived from recipients themselves rather than transplant grafts.

To get a comprehensive functional portrait of MAIT cells in liver transplant recipients, we compare 5-OP-RU/MR1-expanded eMAIT-LT from the recipients at around 1 month post liver transplantation and those expanded from HD (eMAIT-HD) and liver failure patients (eMAIT-LF). eMAIT-LT was clustered together with eMAIT-HD but showed a clear segregation from eMAIT-LF (Fig. 7B, and Supplementary Data 5.4). Although both eMAIT-LF and eMAIT-LT had elevated tissue regeneration capacity, eMAIT-LF upregulated while eMAIT-LT downregulated pro-fibrosis and pro-inflammatory signatures (Fig. 7C, Supplementary Fig. 15B, Supplementary Data 5.5, 6.5). These results suggested that TCR-mediated expansion of MAIT cells would aggravate inflammation-related pathogenic injury and fibrosis in the liver failure patients, but favored tissue regeneration with limited systemic pro-inflammatory potential in the liver transplant recipients. Similar to eMAIT-HD, eMAIT-LT was equipped with comparative transcript levels of IFN-γ, TNF, and granzymes, which were much lower in eMAIT-LF (Fig. 7D, Supplementary Fig. 15C, and Supplementary Data 5.5). These were consistent with

https://doi.org/10.1038/s41467-025-59308-x

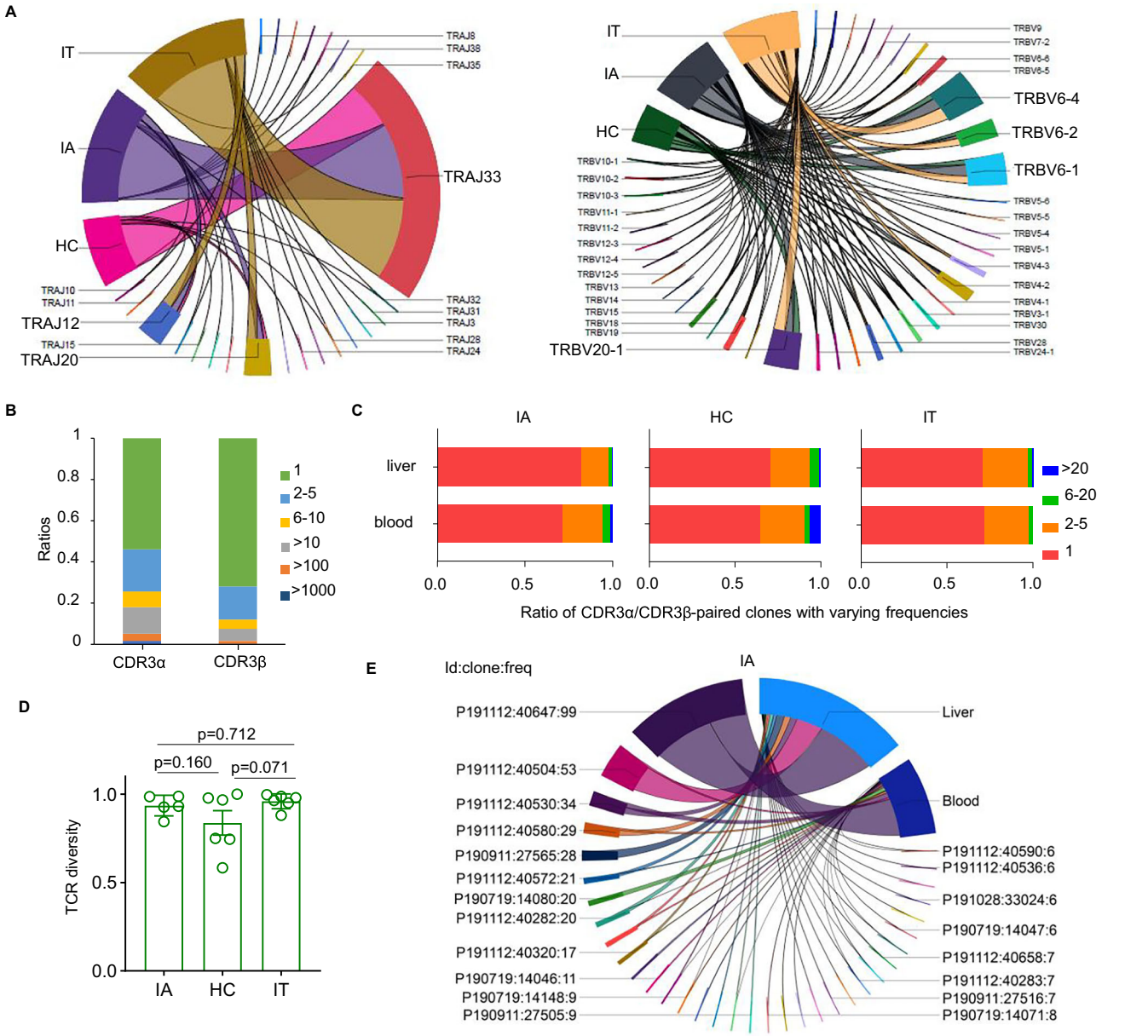

Fig. 5 | TCR usages and overlapping TCR clonotypes of circulating and hepatic MAIT cells. TCR usages and clonotypes of MAIT cells were analyzed among immune active (IA, $n = 5$), immune tolerance (IT, $n = 6$), and healthy control (HC, $n = 6$) groups sourced from dataset GSE182159. **A** Chord diagrams depict TRAJ and TRBV usages of MAIT cells defined by TRAV1-2$^+$SLC4A10$^+$ in the indicated groups. **B** The bar graph, featuring different colors, depicts the ratios of clones with varying frequencies of identical CDR3α or CDR3β sequences. **C** The bar graphs depict ratios of clones with varying frequencies of identical paired CDR3α and CDR3β sequences in both blood and liver of the indicated groups. **D** TCR diversity assessed by the Shannon equitability index in IA ($n = 5$), HC ($n = 6$), and IT ($n = 6$) groups. Data are presented as mean ± SEM. n-values represent biological replicates. Statistical significance was assessed by a one-way ANOVA test followed by Fisher's LSD test. Source data are provided as a Source Data file. **E** The chord diagrams show the frequencies of the liver-blood sharing TCR clonotypes among MAIT cells with clonal frequency over 5 in the indicated groups with patient ID, Clone name, and clone frequency (ID:Clone:Freq) of each clonotypes as axis labels.

the restored IFN-γ producing capacity and TCR-dependent responsiveness of MAIT cells in liver transplant recipients (Fig. 3C, E). In addition, upregulation of CCR6 and CXCR6 were observed in eMAIT-LT compared to eMAIT-LF (Fig. 7D), suggesting their rescued liver homing ability. Therefore, proper activation of MAIT cells by MR1-restricted ligands, like microbially derived metabolites, probably contributes to pathogen control and liver homeostasis post-transplantation.

The restored circulating MAIT cells are associated with favorable clinical outcome

To evaluate the relationship between circulating MAIT cells and liver injury, we conducted Spearman's rank correlation analysis on the MAIT cell frequency and serum biological markers associated with liver function. The frequencies of circulating MAIT cells in liver transplant recipients exhibited an inverse correlation with elevated serum transaminase and bilirubin levels indicative liver injury (Fig. 8A). Conversely, the frequency was positively associated with higher levels of serum total protein reflecting proper liver function. It was noteworthy that CD8$^+$ non-MAIT cells displayed little correlation with these biomarkers (Supplementary Fig. 16A). These data suggested that MAIT cells functioned as a more sensitive sensor to hepatic injury compared to other CD8$^+$ T cells.

Liver transplant carries a risk of a set of complications, including biliary stenosis, hypohepatia, and rejection of the donated liver,

https://doi.org/10.1038/s41467-025-59308-x

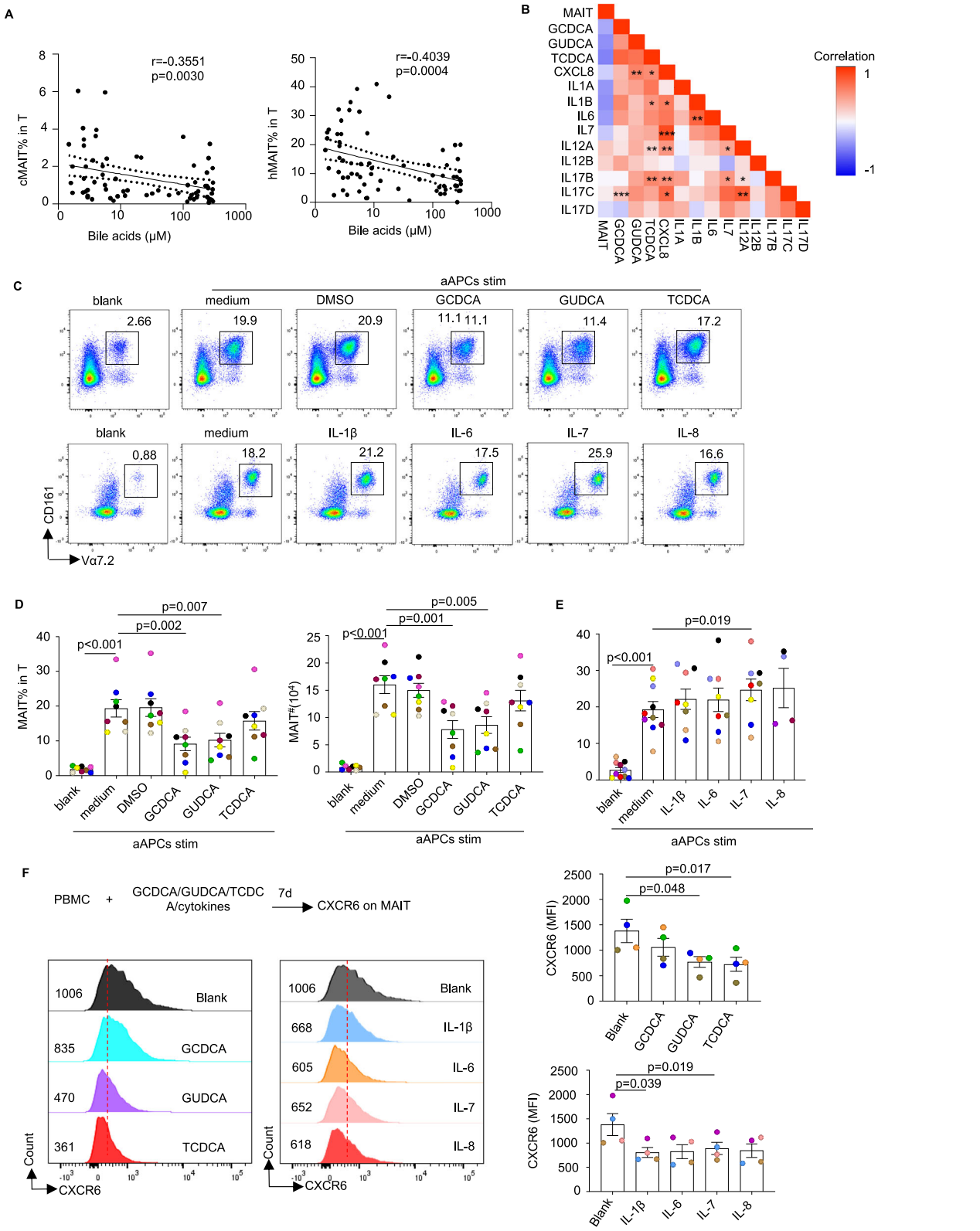

leading to significant morbidity and mortality post liver transplantation. In the current study, 28 recipients under routine anti-rejection drug regimens were followed up for monitoring MAIT cell frequency and long-term complications (Fig. 8B). Among them, 16 recipients exhibited a significant increase in MAIT cell frequency and number within the first month post-liver transplant, experiencing minimal complications during subsequent monitoring (Fig. 8C). Nonetheless, 12 recipients faced substantial complications beyond the 2-month posttransplant period, displaying comprised MAIT cell recovery preceding the onset of adverse effects (Fig. 8D). The increase in both the ratio and number of cMAIT-LT was more strikingly in patients without complications compared to those with complications (Fig. 8E). Despite increases in circulating T cells and $CD8^+$ non-MAIT cells following liver transplantation, there were minimal differences in the rates of increase between groups with and without complications (Supplementary Fig. 16B and C). Thus, the circulating MAIT cell frequency emerges as a

https://doi.org/10.1038/s41467-025-59308-x

Fig. 6 | Bile acid components and pro-inflammatory cytokines dampen the expansion and/or CXCR6 expression of MAIT cells. A Spearman's correlation between the serum bile acids levels with frequencies of cMAIT ($n = 68$) and hMAIT ($n = 72$). Data were collected from at least ten independent experiments and are presented as mean ± SEM. **B** Correlation heatmap depict the relationships between hMAIT frequencies with hepatic bile acids levels and transcript levels of pro-inflammatory cytokines in liver tissue from hMAIT-LF ($n = 5$), hMAIT-HBVN ($n = 4$), and Comp (n = 5), with colors showing correlation index levels. **C** Representative dot plots of the frequencies expanded MAIT cells in the presence of glycochenodeoxycholic acid (GCDCA), glycoursodeoxycholic acid (GUDCA), taurochenodesoxycholic acid (TCDCA), IL-1β, IL-6, IL-7, IL-8. **D** The summarized graph of the frequencies and numbers of expanded MAIT cells in the blank and aAPCs with medium, DMSO ($n = 8$), GCDCA, GUDCA, TCDCA ($n = 8$/group). Data were collected from eight independent experiments and are presented as mean ± SEM. One color in different groups represents the same donor. Statistical significance was assessed by one-way ANOVA multiple comparisons. **E** The summarized graph of the frequencies expanded MAIT cells in the blank ($n = 10$) and aAPCs with medium ($n = 10$), IL-1β ($n = 8$), IL-6 ($n = 8$), IL-7 ($n = 8$), IL-8 ($n = 4$). Data were collected from eight independent experiments and are presented as mean ± SEM. One color in different groups represents the same donor. Statistical significance was assessed by one-way ANOVA multiple comparisons. **F** Representative and summarized CXCR6 levels on MAIT cells in the presence/absence of indicated bile acids or cytokines ($n = 4$/group). Data were collected from four independent experiments. Data are presented as mean ± SEM. *n*-values represent biological replicates. Statistical significance was assessed by one-way ANOVA multiple comparisons. Source data are provided as a Source Data file.

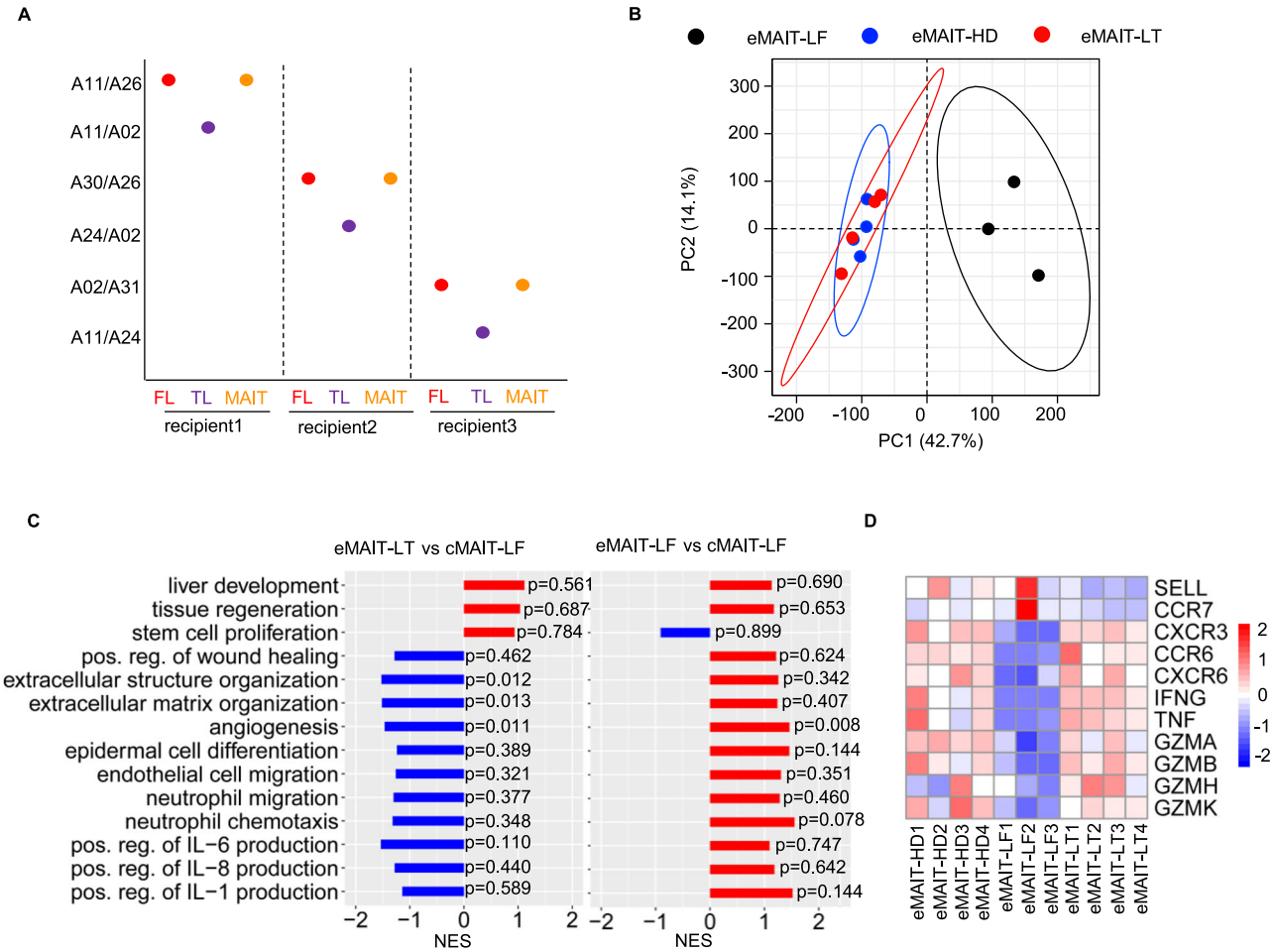

Fig. 7 | Recipient-derived circulating MAIT cells are recovered with protective potential post liver transplantation. A The HLA-A alleles in failure liver (FL) from liver failure patients, and transplanted liver (TL) and eMAIT-LT from 3 recipients. **B** PCA clustering plots for transcripts of 5-OP-RU/MR1-expanded MAIT cells from LT recipients (eMAIT-LT, $n = 4$), HD (eMAIT-HD, $n = 4$), and liver failure patients (eMAIT-LF, $n = 3$). **C** NES values of tissue regeneration-, pro-fibrosis-, and pro-inflammation-related biological processes by GSEA-GO analysis in indicated groups. **D** Heatmap displays the transcript levels of indicated genes across the specific samples, with color gradients representing the relative expression levels.

more sensitive makers than conventional T cells for predicting clinical outcome post liver transplantation. A deficiency in MAIT cell recovery is associated with a heightened risk of long-term complications, whereas the restoration within the initial month post liver transplantation is indicative of a more favorable outcome.

Discussion

MAIT cells are highly enriched and actively patrolling in the human liver. Here, we highlight intensive interaction between MAIT cells and the hepatic environment in liver failure patients and following liver transplantation. In the context of HBV-related liver failure, MAIT cells are severely depleted and dysregulated with pathogenic pro-inflammatory potential and dampened anti-viral capacity. Liver transplantation, rebuilding hepatic homeostasis, refreshes recipient-originated MAIT cells with rectified protective function. The depletion degree and recovery of MAIT cells are associated with disease severity and clinical outcome in liver failure and post-liver transplantation, respectively. Of note, most of the conclusions drawn in this

https://doi.org/10.1038/s41467-025-59308-x

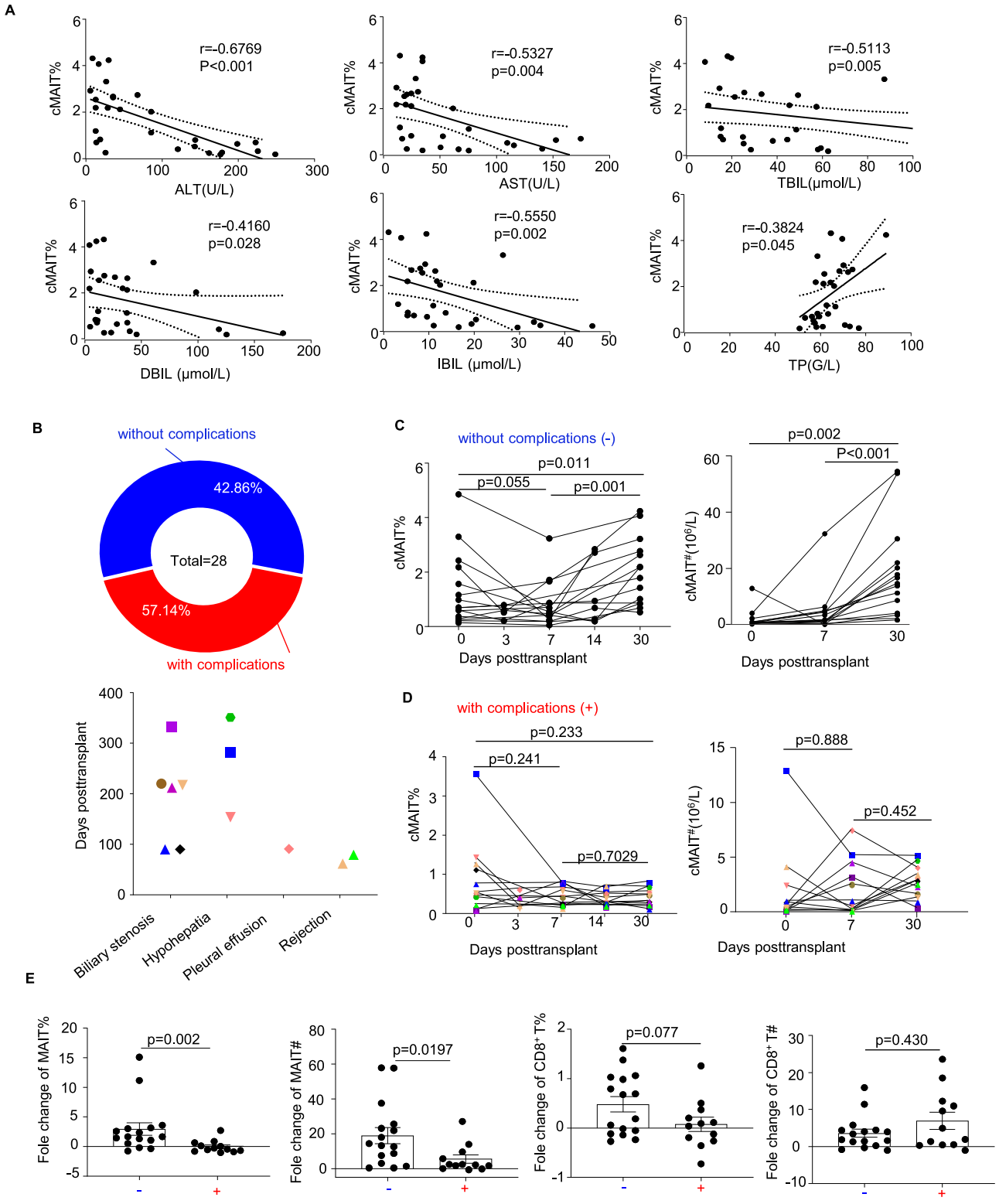

study are based on CD161⁺Vα7.2⁺ cells, and some contamination of non-MAIT T cells cannot be excluded in CD161/Vα7.2 gating. However, we observed consistent trends in MAIT cell ratio changes in LF patients across both approaches. This indicates that, despite the broader scope of anti-CD161/Vα7.2 gating, its findings align closely with those obtained through MR1 tetramer staining in this study.

Recent studies indicate that tissue-derived MAIT cells differ from circulating ones in regard to cell metabolism, activation status, and functional properties[33,40]. However, circulating and hepatic MAIT cells in HBV-related liver failure patients display a similarly dysregulated pattern, including severe defects in frequency, enhanced pathologic pro-inflammatory profiles, and impaired anti-viral potential. MAIT cells have the ability to migrate based on the expression of tissue-homing receptors and the location of transmembrane adhesion molecules. Among which, CCR6, CXCR6 and integrin αEβ7 guide MAIT cells to the bile ducts, and CXCR3, LFA-1 and VLA-4 direct them to the hepatic sinusoids[41–43]. Recent studies show that human MAIT cells exit tissues and recirculate via lymph at steady state, even though they have a low

Fig. 8 | The restored circulating MAIT cells indicate favorable clinical outcome. **A** Spearman correlation between the frequencies of circulating MAIT cells from the recipients posttransplant and the serum levels of indicated clinical parameters (Alanine aminotransferase (ALT($n = 28$)), Aspartate aminotransferase (AST($n = 28$)), Total bilirubin (TBIL($n = 28$)), Direct bilirubin (DBIL($n = 28$)), Indirect bilirubin (IBIL($n = 28$)), Total protein (TP, ($n = 28$))). Data were collected from twenty-eight independent experiments and are presented as mean ± SEM. **B** The proportion of the recipients with ($n = 12$) or without ($n = 16$) complications (**upper panel**) and the types of complications and occurrence days posttransplant are depicted in the right panel by scatter plot (**lower panel**). Different colored symbols indicate distinct individuals in those with complications. **C** Dynamic changes of frequencies (%, 0 d($n = 16$), 3 d($n = 4$), 7 d($n = 16$), 14 d($n = 8$), 30 d($n = 16$)) and number (#, $n = 15$/time point) of cMAIT-LT in patients without complications. Statistical significances are statistically analyzed by a two-tailed paired Student's t test. **D** Dynamic changes of frequencies (%, 0 d ($n = 12$), 3 d ($n = 5$), 7 d ($n = 12$), 14 d ($n = 12$), 30 d ($n = 12$)) and number (#, $n = 12$/time point) of cMAIT-LT in patients with complications. Different colored symbols indicate distinct individuals in those with complications. Statistical significances are statistically analyzed by a two-tailed paired Student's t test between each pair of two groups. **E** The change rate of MAIT cells and $CD8^+$non-MAIT cells frequencies and numbers at 30-day posttransplant compared with day 0 was depicted by scatter graphs with complications ($n = 12$)/without complications ($n = 16$). Data were collected from twenty-eight independent experiments and are presented as mean ± SEM. n-values represent biological replicates. Statistical significance was statistically analyzed by the Mann-Whitney test. Source data are provided as a Source Data file.

level of CCR7 and CD62L expression[34,44]. This can partially explain the rather high frequency of MAIT cells in peripheral blood. There are cMAIT cells with transcriptomic similarity to hMAIT, as well as significant TCR overlaps in circulating and hepatic MAIT cells from HBV-infected patients with liver injury. This suggests that circulating and hepatic MAIT cells either encounter similar differentiation or have enhanced trafficking during liver injury status. Of note, the downregulated homing receptors like CXCR6 and CCR6 of MAIT cells in liver failure patients, which were upregulated post liver transplantation, indicate a change of migration profile of MAIT cells during liver disease or healthy status. Given that the recovered circulating MAIT cells are derived from recipients rather than transplanted grafts after liver transplantation, it is reasonable to propose that hepatic factors should affect MAIT cell trafficking and refresh. However, the MAIT cell trafficking in the patients and the refresh mechanism of MAIT cells in the recipients need to be further investigated.

Lower frequency of circulating and hepatic MAIT cells was coincident with more serious liver pathology in LF patients and multiple complications, suggesting clinical significance of MAIT cell dysregulation in disease progression. MAIT cells have now been widely assessed in chronic viral hepatitis[5,23], alcoholic liver disease[8], and different types of autoimmune liver diseases[27,28]. Given that MAIT cells harbor anti-microbial[8,9], tissue repair[13,14], and pro-fibrosis potential[45,46], their roles during liver injury and liver regeneration are supposed to be intricate. Clarifying the precise disease-related roles of MAIT cells and determining the factors directing their functionality provides therapeutic implications and predicative value in HBV-related liver failure and subsequent liver transplantation. Dysregulated MAIT cells in liver failure patients increase IL-17 producing capacity and IL-1/IL-6/IL-8 production processes, which is supposed to aggravate inflammation-associated liver injury[47]. Accumulated primary bile acids in failure liver not only impairs TCR-mediated MAIT cell expansion but also promotes its pro-inflammatory cytokines production, suggesting hepatic metabolic targets to prevent MAIT cell dysregulation. Aberrant tissue repair potential with enhanced systemic pro-inflammatory signature in MAIT cells from liver failure patients was additionally enhanced by 5-OP-RU/MR1 specific activation. However, 5-OP-RU/MR1-activated MAIT cells from LT recipients show tissue regeneration potency with low pro-inflammatory tendency. Therefore, apart from liver transplantation, synchronous targeting hepatic environment and dysregulated MAIT cells should be considered for the immunotherapy strategy against inflammation-related liver injury.

Little change in cell ratio and IFN-γ-producing capacity of MAIT cells was observed in liver transplant patients receiving various Tacrolimus dosages and other combined immunosuppression drugs, indicating that different immunosuppression therapy regimens have little impact on MAIT cells. Given that the main difference lies in the degree of liver injury between LF patients and the recipients, liver damage-associated environmental factors are supposed to be involved in the dysregulation of MAIT cells. Supportively, conjugated bilirubin is revealed as a critical factor for dysregulation of MAIT cells frequency and function in chronic HBV-infected patients. Here, accumulated primary bile acids (TCDCA, GCDCA) and secondary bile acids produced by bacterial modification (GUDCA, DCA, UDCA) in failure liver not only impair TCR-mediated MAIT cell expansion but promote its pro-inflammatory cytokines production. Notably, bile acids-mediated CXCR6 downregulation possibly contributes to the enhanced recirculation of MAIT cells in liver failure patients. These underscores the intense interaction between MAIT cells and the challenging hepatic environment and indicate the involvement of bile acids-dysregulated MAIT cells in promoting liver inflammation, which provides targets to further improve current MAIT cell-based management strategies[48].

Under certain circumstances, inappropriate tissue repair activity of MAIT cells is involved in fibrosis and potentially promotes tumor growth[15]. Here, aberrant tissue repair potential with enhanced systemic pro-inflammatory signature in MAIT cells from LF patients was additionally enhanced by 5-OP-RU/MR1-specific activation. However, 5-OP-RU/MR1-activated MAIT cells from liver transplantation recipients show tissue regeneration potential with low pro-inflammatory tendency. These indicate that TCR-mediated activation aggravates the inflammation-related injury potential of dysregulated MAIT cells in LF patients, but favor the protective function of restored MAIT cells from liver transplantation recipients. Vitamin-related metabolites originating from the microbiota and drug-related metabolites resulting from liver metabolism have been identified as MAIT cell-reactive ligands. Therefore, MAIT cells are capable to be activated in a TCR-dependent manner in vivo through these ligands. The ample number and function of MAIT cells in liver transplant recipients is supposed to be activated in a proper way with protective effects. Consistent with this, sufficient MAIT cell recovery post liver transplantation suggests a favorable clinical outcome.

In summary, MAIT cell recovery from severe dysregulation in liver failure patients following liver transplantation suggests three key clinical implications. Firstly, MAIT cells exhibit intensive interactions with the hepatic microenvironment, and the frequency and functional status of MAIT cells correlate with disease prognosis in liver failure patients and following liver transplantation. Secondly, MAIT cells serve as early sensors for changes in the hepatic microenvironment, including bile acid and biomarkers indicating liver injury. Finally, the restored MAIT cells, endowing with enhanced tissue repair and reduced inflammatory potential, contribute to liver healthy, supported by sufficient MAIT cell recovery with a favorable clinical outcome. Therapeutic strategies directed at reducing distinct bile acids and restoring liver hemostasis, rather than elimination of a prime pathogenic factor, may effectively recover their protective function and alleviate MAIT cell-related liver inflammation.

Methods

Patients and samples

Blood samples were collected from a total of 292 heathy donors and 287 patients infected with HBV-infected patients. Within the HBV-infected group, 180 exhibited compensated liver function, while 107

were diagnosed with liver failure who received artificial liver support system ($n = 61$) or liver transplant ($n = 46$) in Tongji Hospital, Wuhan, China. 42 liver specimens were collected from patients experiencing liver failure underwent liver transplant procedures. 4 biopsy samples were obtained approximately two weeks post-transplantation. Control liver tissues were obtained from two distinct groups during hepatic resection: 70 HBV-infected patients with hepatic carcinoid ($n = 8$) or hepatocellular carcinoma ($n = 62$), and 50 HBV-negative patients with benign hepatic cyst or hemangioma.

To ensure the specificity of the study, individuals with other concurrent types of viral hepatitis, HIV, autoimmune liver disease, or alcohol-associated liver disease were excluded. A comprehensive summary of the characteristics of all enrolled patients is presented in Table 1, and clinical details and sample information of LF individuals are listed in Supplementary Data 2.

Study approval

This study was approved by the human research committee of Tongji Medicine College, Huazhong University of Science and Technology (reference number 2023S064). Written informed consent to publish clinical information was obtained prior to participation from each patient included in the study.

Immune cell isolation and Flow Cytometry

Peripheral blood mononuclear cells (PBMCs) were isolated by Ficoll density gradient centrifugation, and intrahepatic mononuclear cells were isolated by a modified enzymatic dispersal protocol followed by Percoll density purification[5]. Phenotypes and function of isolated immune cells were detected by the following antibodies from BioLegend, including anti-human CD45, anti-human CD3, anti-human CD8, anti-human TCRVα7.2, anti-human CD161, anti-human IFN-γ, anti-human TNF, anti-human IL-17A, and anti-human CCR6. BV421-labeled 5-OP-RU/MR1 tetramer-stained circulating and hepatic MAIT cells, and PerCP-Cy5.5-conjugated CD8-stained $CD8^+$ T cells were flow cytometry sorted by FACS Aria III (BD Bioscience). PBMCs or intrahepatic mononuclear cells were stimulated by phorbol-12-myristate-13-acetate (PMA, 25 ng/mL)/ionomycin (Ion, 500 ng/mL), followed by a 3.5 h incubation with brefeldin A, surface staining, fixation/permeabilization, and intracellular staining with antibodies against IFN-γ and IL-17A[5]. Data were collected using FACSVerse (BD Bioscience) and analyzed by FlowJo software (Tree Star). The conjugated fluorochrome, clone number, catalog number, and/or dilutions of all the reagents are listed in Supplementary Data 1.

Disease severity and histology assessment

Score of Model for End-stage Liver Disease (MELD), a commonly used metric to assess severity of liver diseases, was calculated as follows[49]: $9.57 \times \log_e$ (creatinine mg/dL) $+ 3.78 \times \log_e$ (bilirubin mg/dL) $+ 11.2 \times \log_e$ (international normalized ratio (INR)) $+ 6.43$. Liver specimens were fixed in 4% paraformaldehyde, embedded in paraffin, and sectioned. Hematoxylin-Eosin staining was performed, and the whole section were scanned by Pannoramic MIDI (3D HISTECH) for histopathology assessment of liver tissue. Histological activity index (HAI), was evaluated according periportal bridging necrosis, intralobular degeneration, focal necrosis, portal inflammation and fibrosis. Clinical details, including MELD scores, HAI values, therapy drug employed, and complications of LF patients underwent artificial liver support system and liver transplantation were listed in Supplementary Data 2.

MAIT cell expansion and treatment

PBMCs from healthy donors, LF patients, and liver transplant recipients were stimulated with artificial antigen-presenting cells (aAPCs) coating with 5-OP-RU/MR1 tetramer and anti-CD28 antibodies for 7days[5]. The cultured PBMCs were then collected for flow cytometry analysis or sorted MAIT cells by flow cytometry for RNA-sequencing.

PBMCs from healthy donors were stimulated with 5-OP-RU/MR1 aAPCs in the presence of intervention reagents including GCDCA (50 μM, MCE), GUDCA (50 μM, MCE), TCDCA (50 μM, MCE), IL-1β (10 ng/mL, PeproTech), IL-6 (50 ng/mL, PeproTech), IL-7 (50 ng/mL, PeproTech), or IL-8 (50 ng/mL, PeproTech). PBMCs without stimulation were served as blank controls. The supernatant from culture system were collected to detect the cytokines such as IFN-γ, IFN-α2, MCP-1, IL-6, IL-33, IL-23, IL-8, IL-10, IL-12P70, IL-17A, IL-18, IL-1β, TNF. The concentration of cytokine was detected through flow cytometry by Human Inflammation Panel 1 (Biolegend Cat.NO.740808). The frequency, Annexin V positively stained cells and CXCR6 levels of MAIT cells were checked through flow cytometry. The inhibitory rate of various reagents on the expansion of MAIT cells was calculated as follows: $(MAIT\%^{\text{without BA}} - MAIT\%^{BA})/(MAIT\%^{\text{without BA}} - MAIT\%^{\text{Blank}})$.

RNA sequencing and data analysis

Homogenized liver tissue and flow cytometry sorted MAIT cells from blood and liver of the patients and controls (Supplementary Data 3) were subscribed to RNA extraction for stranded RNA sequencing library preparation and reads mapping to the reference genome using STAR software (version 2.5.3a) and counted by featureCounts (Subread-1.5.1;Bioconductor)[5]. Principal component analysis (PCA) was performed and differentially expressed genes (DEGs) between groups were identified using the DESeq2 package (version 1.32.0). Gene ontology (GO) analysis and Gene set enrichment analyses (GSEA) enrichment analysis with normalized enrichment score (NES) were perfomed and visualization to screening distinct biological processes and associated genes to produce bar graphs and heatmaps with the clusterProfiler and pheatmap packages in R (R Foundation for Statistical Computing,

Table 1 | Clinical characteristic of Patients Enrolled in this Study

	blood		Nontumor Liver Specimens		
samples	Comp	LF	HBVN	Comp	LF
NO.	180	107	50	70	42
Sex(M/F)	126/54	87/20	26/24	58/12	36/6
Age(year)*	47(36–58)	47(37–57)	49(35–63)	50(40–60)	46(36–56)
HBV-DNA, $\log_{10}$copies/mL#	2.7(2.7–3.94)	4.6(2.8–6.1)	ND	3.2(2.0–5.0)	5.3(2.6–6.8)
ALT(U/L)#	26(19–43)	70(36–244)	16(11–30)	27(18–42)	53(31–413)
AST(U/L)#	25(21–37)	95(50–246)	19.5(15–25)	28.5(22–42.2)	92(49.5–451.5)
BA(μmol/L)#	5.2(2.8–11.1)	179(151–279)	4.2(2.5–6.4)	4.0(2.5–7.8)	236(134–278)
TBIL(μmol/L)#	13.4(10.4–18.5)	290(164–432)	11.3(6.8–16.6)	13.2(8.9–18.8)	236(90–412)

ND not determined. Alanine aminotransferase (ALT), Aspartate aminotransferase (AST), Bile acid (BA), Total bilirubin (TBIL). Data are shown as mean (range)* or median (range)#

Vienna, Austria). TCR repertoire was mined by MiXCR software (available at https://github.com/milaboratory/mixcr/)[50]. HLA allele genotyping to define the donor or recipient origin of MAIT cells was performed using arcas-hla software with bulk RNA sequencing data of liver specimens and sorted MAIT cells (available at https://github.com/RabadanLab/arcasHLA[51].

Single-cell RNA-seq data reanalyzing

The published single-cell RNA sequencing dataset for secondary analysis was accessible under the accession number GSE182159[36]. Three groups with paired liver and blood samples were enrolled in this study, including 5 HBV-infected patients in an immune active (IA) characterized by abnormal liver necroinflammation, fibrosis and serum ALT level, 6 HBV-infected patients in an immune tolerance (IT) state characterized by high-serum HBV DNA but normal serum ALT and mostly normal liver histology status and 6 HBV-free healthy controls (HC). MAIT cells were identified based on canonical markers TRAV1-2 and SLC4A10. PCA, uniform manifold approximation and projection (UMAP) clustering, and DEGs analysis were performed using the R package Seurat (https://satijalab.org/seurat/). The DEGs between circulating MAIT cells from IA and IT patients with adjusted *P*-value lower than 0.05 were selected for GO biological processes enrichment using the clusterProfiler package, and the top 20 processes with the lowest *P*-value were visualized using ggplot2. TCR usage mapping was visualized using Power BI desktop with Chord diagrams to illustrate the distribution and frequency of TCR clonotypes.

Nontargeted metabolomics analysis

The sample stored at − 80 °C refrigerator was thawed on ice. The thawed sample was homogenized by a grinder (30 HZ) for 20 s. A 400 µL solution (Methanol: Water = 7:3, V/V) containing internal standard was added in to 20 mg grinded sample and shaked at 1500 rpm for 5 min. After placing on ice for 15 min, the sample was centrifuged at 12000 rpm for 10 min (4 °C). A 300 µL of supernatant was collected and placed in − 20 °C for 30 min, and then centrifuged at 12000 rpm for 3 min (4 °C). 200 µl aliquots of supernatant were transferred for LC-MS/MS analysis by Wuhan Metware Biotechnology Co., and data were converted into mzML format by ProteoWizard software. Peak extraction, peak alignment, and retention time correction were, respectively, obtained by the XCMS program. PCA for metabolite components and orthogonal projections to latent structures discriminate analysis (OPLSDA) for differential metabolite analysis were performed using the R package ropls. Differential metabolites between groups were determined by VIP (VIP ≥ 1), *P*-value (*P*-value < 0.05, Student's *t* test), and absolute Log_2FC ($|Log_2FC| \geq 1.0$). The top 5% differentially abundant metabolites between the patient groups are listed in Supplementary Data 4.

Statistical analysis

Data with normal distribution and equal variance were analyzed using the Student's *t* test for two-group comparisons or ANOVA for three or more groups, followed by Fisher's LSD test by GraphPad Prism software (version 8.0). For non-normally distributed variables, the Mann-Whitney U test was used for two-group comparisons, and the Kruskal-Wallis test with Dunns' post-hoc test was applied for comparisons of multiple groups. Correlation analysis was assessed by Spearman's rank correlation. *P*-values < 0.05 were considered statistically significant (*$P < 0.05$; **$P < 0.01$; ***$P < 0.001$).

Reporting summary

Further information on research design is available in the Nature Portfolio Reporting Summary linked to this article.

Data availability

The transcript data discussed in this publication have been deposited in NCBI's Gene Expression Omnibus and are accessible through GEO Series accession number GSE222856 for the transcriptome of liver tissues and number GSE223075 for the transcriptome of FACS-sorted MAIT and $CD8^+$ non-MAIT cells. Sample details were listed in Supplementary Data 3. Statistical details of DEGs from various group comparisons are provided in Supplementary Data 5.1 to Supplementary Data 5.5, and the statistical details of NES values for enriched pathways are listed in Supplementary Data 6.1 to Supplementary Data 6.5. All data are included in the Supplementary Information or available from the authors, as are unique reagents used in this Article. The raw numbers for charts and graphs are available in the Source Data file whenever possible. Source data are provided in this paper.

Code availability

The codes generated during this study are available at Zenodo (https://zenodo.org/records/15105789, https://doi.org/10.5281/zenodo.15105789).

References

1. Bernal, W., Auzinger, G., Dhawan, A. & Wendon, J. Acute liver failure. *Lancet* **376**, 190–201 (2010).
2. Sarin, S. K. et al. Acute-on-chronic liver failure: consensus recommendations of the Asian Pacific association for the study of the liver (APASL): an update. *Hepatol. Int* **13**, 353–390 (2019).
3. Ginès, P. et al. Liver cirrhosis. *Lancet* **398**, 1359–1376 (2021).
4. Klugewitz, K., Blumenthal-Barby, F., Eulenburg, K., Emoto, M. & Hamann, A. The spectrum of lymphoid subsets preferentially recruited into the liver reflects that of resident populations. *Immunol. Lett.* **93**, 159–162 (2004).
5. Liu, Y. et al. Mucosal-associated invariant T cell dysregulation correlates with conjugated bilirubin level in chronic HBV infection. *Hepatology* **73**, 1671–1687 (2021).
6. Gibbs, A. et al. MAIT cells reside in the female genital mucosa and are biased towards IL-17 and IL-22 production in response to bacterial stimulation. *Mucosal Immunol.* **10**, 35–45 (2017).
7. Kjer-Nielsen, L. et al. MR1 presents microbial vitamin B metabolites to MAIT cells. *Nature* **491**, 717–723 (2012).
8. Riva, A. et al. Mucosa-associated invariant T cells link intestinal immunity with antibacterial immune defects in alcoholic liver disease. *Gut* **67**, 918–930 (2018).
9. Tastan, C. et al. Tuning of human MAIT cell activation by commensal bacteria species and MR1-dependent T-cell presentation. *Mucosal Immunol.* **11**, 1591–1605 (2018).
10. van Wilgenburg, B. et al. MAIT cells are activated during human viral infections. *Nat. Commun.* **7**, 11653 (2016).
11. Boeijen, L. L. et al. Mucosal-associated invariant T cells are more activated in chronic hepatitis B, but not depleted in blood: Reversal by antiviral therapy. *J. Infect. Dis.* **216**, 969–976 (2017).
12. Zhang, Y. et al. Mucosal-associated invariant T cells restrict reactive oxidative damage and preserve meningeal barrier integrity and cognitive function. *Nat. Immunol.* **23**, 1714–1725 (2022).
13. Constantinides, M. G. et al. MAIT cells are imprinted by the microbiota in early life and promote tissue repair. *Science* **366**, https://doi.org/10.1126/science.aax6624 (2019).
14. Leng, T. et al. TCR and Inflammatory signals tune human MAIT cells to exert specific tissue repair and effector functions. *Cell Rep.* **28**, 3077–3091.e3075 (2019).
15. Salou, M. & Lantz, O. A TCR-Dependent tissue repair potential of MAIT cells. *Trends Immunol.* **40**, 975–977 (2019).
16. Niehaus, C. E. et al. MAIT Cells are enriched and highly functional in ascites of patients with decompensated Liver Cirrhosis. *Hepatology* **72**, 1378–1393 (2020).

17. Keller, A. N. et al. Drugs and drug-like molecules can modulate the function of mucosal-associated invariant T cells. *Nat. Immunol.* **18**, 402–411 (2017).
18. Godfrey, D. I., Koay, H.-F., McCluskey, J. & Gherardin, N. A. The biology and functional importance of MAIT cells. *Nat. Immunol.* **20**, 1110–1128 (2019).
19. Lopez-Sagaseta, J. et al. The molecular basis for Mucosal-Associated Invariant T cell recognition of MR1 proteins. *Proc. Natl. Acad. Sci. USA* **110**, E1771–E1778 (2013).
20. Reantragoon, R. et al. Structural insight into MR1-mediated recognition of the mucosal associated invariant T cell receptor. *J. Exp. Med.* **209**, 761–774 (2012).
21. Rha, M.-S. et al. Human liver CD8+ MAIT cells exert TCR/MR1-independent innate-like cytotoxicity in response to IL-15. *J. Hepatol.* **73**, 640–650 (2020).
22. Faitot, F. et al. Metabolomic profiling highlights the metabolic bases of acute-on-chronic and post-hepatectomy liver failure. *HPB* **21**, 1354–1361 (2019).
23. Dias, J. et al. Chronic hepatitis delta virus infection leads to functional impairment and severe loss of MAIT cells. *J. Hepatol.* **71**, 301–312 (2019).
24. Bolte, F. J. et al. Intra-hepatic depletion of mucosal-associated invariant T cells in hepatitis C virus-induced Liver inflammation. *Gastroenterology* **153**, 1392–1403.e1392 (2017).
25. Yan, J. et al. MAIT Cells promote tumor initiation, growth, and metastases via tumor MR1. *Cancer Discov.* **10**, 124–141 (2020).
26. Duan, M. et al. Activated and exhausted MAIT cells foster disease progression and indicate poor outcome in hepatocellular Carcinoma. *Clin. Cancer Res.* **25**, 3304–3316 (2019).
27. Jiang, X. et al. The immunobiology of mucosal-associated invariant T cell (MAIT) function in primary biliary cholangitis: Regulation by cholic acid-induced Interleukin-7. *J. Autoimmun.* **90**, 64–75 (2018).
28. Bottcher, K. et al. MAIT cells are chronically activated in patients with autoimmune liver disease and promote profibrogenic hepatic stellate cell activation. *Hepatology* **68**, 172–186 (2018).
29. Carbone, F. R. Tissue-resident memory T cells and fixed immune surveillance in nonlymphoid organs. *J. Immunol.* **195**, 17–22 (2015).
30. Wakim, L. M., Waithman, J., van Rooijen, N., Heath, W. R. & Carbone, F. R. Dendritic cell-induced memory T cell activation in nonlymphoid tissues. *Science* **319**, 198–202 (2008).
31. Kumar, B. V. et al. Human tissue-resident memory T cells are defined by core transcriptional and functional signatures in lymphoid and mucosal sites. *Cell Rep.* **20**, 2921–2934 (2017).
32. Cortez, V. S. et al. CRTAM controls residency of gut CD4+CD8+ T cells in the steady state and maintenance of gut CD4+ Th17 during parasitic infection. *J. Exp. Med.* **211**, 623–633 (2014).
33. Slichter, C. K. et al. Distinct activation thresholds of human conventional and innate-like memory T cells. *JCI Insight* **1**, https://doi.org/10.1172/jci.insight.86292 (2016).
34. Voillet, V. et al. Human MAIT cells exit peripheral tissues and recirculate via lymph in steady state conditions. *JCI Insight* **3**, https://doi.org/10.1172/jci.insight.98487 (2018).
35. Sattler, A. et al. Mucosal associated invariant T cells are differentially impaired in tolerant and immunosuppressed liver transplant recipients. *Am. J. Transpl.* **21**, 87–102 (2021).
36. Zhang, C. et al. Single-cell RNA sequencing reveals intrahepatic and peripheral immune characteristics related to disease phases in HBV-infected patients. *Gut* **72**, 153–167 (2023).
37. Salou, M. et al. A common transcriptomic program acquired in the thymus defines tissue residency of MAIT and NKT subsets. *J. Exp. Med.* **216**, 133–151 (2018).
38. Garner, L. C. et al. Single-cell analysis of human MAIT cell transcriptional, functional and clonal diversity. *Nat. Immunol.* **24**, 1565–1578 (2023).
39. Zhang, L. et al. Runt-related transcription factor-1 ameliorates bile acid-induced hepatic inflammation in cholestasis through JAK/STAT3 signaling. *Hepatology* **77**, 1866–1881 (2023).
40. Lamichhane, R. et al. Human liver-derived MAIT cells differ from blood MAIT cells in their metabolism and response to TCR-independent activation. *Eur. J. Immunol.* **51**, 879–892 (2021).
41. Czaja, A. J. Review article: chemokines as orchestrators of autoimmune hepatitis and potential therapeutic targets. *Aliment Pharm. Ther.* **40**, 261–279 (2014).
42. Jeffery, H. C. et al. Biliary epithelium and liver B cells exposed to bacteria activate intrahepatic MAIT cells through MR1. *J. Hepatol.* **64**, 1118–1127 (2016).
43. Ma, C. A.-O. et al. Gut microbiome-mediated bile acid metabolism regulates liver cancer via NKT cells. *Science* **360**, https://doi.org/10.1126/science.aan5931 (2018).
44. Legoux, F., Salou, M. & Lantz, O. MAIT Cell development and functions: The microbial connection. *Immunity* **53**, 710–723 (2020).
45. Hegde, P. et al. Mucosal-associated invariant T cells are a profibrogenic immune cell population in the liver. *Nat. Commun.* **9**, 2146 (2018).
46. Mehta, H., Lett, M. J., Klenerman, P. & Filipowicz Sinnreich, M. MAIT cells in liver inflammation and fibrosis. *Semin. Immunopathol.* **44**, 429–444 (2022).
47. Kaufmann, B. et al. NLRP3 activation in neutrophils induces lethal autoinflammation, liver inflammation, and fibrosis. *EMBO Rep.* **23**, e54446 (2022).
48. Cui, C. et al. T cell receptor beta-chain repertoire analysis of tumor-infiltrating lymphocytes in pancreatic cancer. *Cancer Sci.* **110**, 61–71 (2019).
49. Wiesner, R. et al. Model for end-stage liver disease (MELD) and allocation of donor livers. *Gastroenterology* **124**, 91–96 (2003).
50. Bolotin, D. A. et al. MiXCR: software for comprehensive adaptive immunity profiling. *Nat. Methods* **12**, 380–381 (2015).
51. Orenbuch, R. et al. arcasHLA: high-resolution HLA typing from RNAseq. *Bioinformatics* **36**, 33–40 (2020).

Acknowledgements

This work was supported by the National Key Research and Development Program of China (2023YFC2308600 to X. Wang/X. Weng), Nature Science Foundation of China NSFC (32170920 and 32370977 to X. Weng), independent project of State Key Laboratory for Diagnosis and Treatment of Severe Zoonotic Infectious Disease (2024ZZ00003 to X. Weng), and Hubei key R&D project (2022BCA015 to Z. Chen). We are grateful for experimental support from the National Institutes of Health (NIH) for the MR1 tetramer loaded with vitamin B derivative 5-(2-oxopropylideneamino)-6-D-ribitylaminouracil (5-OP-RU).

Author contributions

W. Wang, C. Dai, P. Zhu, X. Wu, Z. Chen, and X. Weng conceived and designed the experiments. W. Wang, H. Zhang, M. Wu, J. Weng, X. Cheng, Y. Jiang, and T. Zhou performed the experiments. C. Dai, Q. Wei, X. Tan, and P. Zhu collected clinical samples and provided the characteristics of patients. W. Wang, C. Dai, H. Zhang, Z. Liang, Z. Chen, and X. Weng analyzed the data. W. Wang and X. Weng wrote the manuscript.

Competing interests

The authors declare no competing interests.

Additional information

Supplementary information The online version contains supplementary material available at https://doi.org/10.1038/s41467-025-59308-x.

Correspondence and requests for materials should be addressed to Zhishui Chen or Xiufang Weng.

Peer review information *Nature Communications* thanks Arne Sattler and the other anonymous reviewer(s) for their contribution to the peer review of this work. A peer review file is available.